J Membrane Biol (2007) 215:93–103
DOI 10.1007/s00232-007-9009-0

Studies of Receptor Tyrosine Kinase Transmembrane Domain Interactions: The EmEx-FRET Method

Mikhail Merzlyakov · Lirong Chen · Kalina Hristova

Received: 20 December 2006 / Accepted: 10 January 2007 / Published online: 14 June 2007

Abstract The energetics of transmembrane (TM) helix dimerization in membranes and the thermodynamic principles behind receptor tyrosine kinase (RTK) TM domain interactions during signal transduction can be studied using Förster resonance energy transfer (FRET). For instance, FRET studies have yielded the stabilities of wild-type fibroblast growth factor receptor 3 (FGFR3) TM domains and two FGFR3 pathogenic mutants, Ala391Glu and Gly380Arg, in the native bilayer environment. To further our understanding of the molecular mechanisms of deregulated FGFR3 signaling underlying different pathologies, we determined the effect of the Gly382Asp FGFR3 mutation, identified in a multiple myeloma cell line, on the energetics of FGFR3 TM domain dimerization. We measured dimerization energetics using a novel FRET acquisition and processing method, termed ''emission-excitation FRET (EmEx-FRET),'' which improves the precision of thermodynamic measurements of TM helix association. The EmEx-FRET method, verified here by analyzing previously published data for wild-type FGFR3 TM domain, should have broad utility in studies of protein interactions, particularly in cases when the concentrations of fluorophore-tagged molecules cannot be controlled.

Keywords Receptor tyrosine kinase · Transmembrane domain · FRET

M. Merzlyakov · L. Chen · K. Hristova (✉)
Department of Materials Science and Engineering, Johns Hopkins University, Baltimore, MD 21218, USA
e-mail: kh@jhu.edu

Introduction

The receptor tyrosine kinase (RTK) family comprises a large group of single-pass membrane proteins that conduct biochemical signals upon dimerization in the plasma membrane (Fantl, Johnson and Williams 1993). The dimerization process brings the catalytic domains in close proximity and results in their cross-phosphorylation and activation (Schlessinger 2000; van der Geer, Hunter and Lindberg 1994). RTKs regulate cell growth, differentiation and metabolism; and their deregulation leads to pathologies (Blume-Jensen and Hunter 2001). Functional defects can arise due to chromosomal translocations, protein overexpression or the occurrence of missense gain-of-function mutations. Often, such missense mutations occur in the transmembrane (TM) domains of RTKs. Two mechanisms have been proposed to contribute to pathogenesis due to RTK TM mutations (Li and Hristova 2006; Cho et al. 2004): (1) direct dimer stabilization of the TM domain dimers, mediated by hydrogen bonds, disulfide bonds and cation-π interactions, and (2) defects in the downregulation of the activated receptor dimers in the cell. The relative importance of these two mechanisms in pathogenesis has not been explored in detail. Furthermore, it is not known if a specific mutation can affect both dimer stability and downregulation efficiency. Previously, we characterized the stability of the wild-type (WT) fibroblast growth factor receptor 3 (FGFR3) TM domain dimer (Li, You and Hristova 2005) as well as two pathogenic dimers (Li, You and Hristova 2006; You, Li and Hristova 2006). FGFR3 is an RTK that plays an important role in human skeletal development (Deng et al. 1996), and the studied mutations are associated with skeletal dysplasias. The first one, Ala391Glu, is linked to Crouzon syndrome with

acanthosis nigricans, an autosomal dominant disorder characterized by premature ossification of the skull (craniosynostosis) (Meyers et al. 1995), accompanied by skin hyperpigmentation and thickening (hyperkeratosis), as well as to bladder cancer (van Rhijin et al. 2002). The second one, Gly380Arg, is linked to achondroplasia (Shiang et al. 1994; Webster and Donoghue 1996), the most common form of human dwarfism, characterized by short stature (Vajo, Francomano and Wilkin 2000), and is also found in some cancers (van Rhijin et al. 2002). We have shown that while the Ala391Glu mutation stabilizes the FGFR3 TM domain dimer by –1.3 kcal/mol (Li, You and Hristova 2006; Merzlyakov et al. 2006), the achondroplasia mutation, Gly380Arg, does not alter the stability of the FGFR3 TM domain dimer (You, Li and Hristova 2006).

Such studies of dimerization propensities of isolated RTK TM domains and their pathogenic mutants can provide insights into pathogenesis mechanisms. If the isolated RTK TM dimer is stabilized due to a particular mutation, it could be expected that this mutation stabilizes the active dimeric state of the whole receptor. If, however, the mutation has no effect on TM dimer stability, other mechanisms of pathogenesis, such as slow downregulation of the activated receptors, are likely at play. Therefore, comparative studies of TM dimer stabilities can help us uncover the relative importance of direct stabilization of RTK dimers in various pathologies.

Here, we investigated a Gly382Asp mutant identified in a multiple myeloma cell line (Otsuki et al. 1998). We found that the Gly382Asp mutation does not stabilize the FGFR3 TM dimer. This finding is consistent with a published structural model of the FGFR3 TM domain dimer (Li, You and Hristova 2006), in which Gly382 does not participate in the helix-helix contacts. Therefore, pathogenesis associated with the Gly382Asp mutation is likely not due to dimer stabilization. The exact role of the mutation in multiple myeloma pathogenesis is yet to be identified.

We also present a novel robust Förster resonance energy transfer (FRET) acquisition and processing method that gives the free energy of dimerization of TM helices with high precision. The method that we describe, termed ''emission-excitation FRET'' (EmEx-FRET), relies on the acquisition of both emission and excitation spectra. These two spectra are combined with standard donor-only and acceptor-only emission and excitation spectra to yield the actual donor and acceptor concentration, the FRET efficiency and the free energy of dimerization. We verified the EmEx-FRET method using previously published data for the WT FGFR3 TM domain (Li, You and Hristova 2006) and used it to determine the dimerization energetics of the Gly382Asp mutant.

The EmEx-FRET method presented here provides a tool to efficiently probe the stability of TM helix dimers, including RTK TM domain dimers and their pathogenic mutants. The method reduces experimental uncertainties due to sample-to-sample variations in protein concentrations as a result of the very low solubility of the hydrophobic TM helices. In addition, this method can have broad utility when the concentrations of the donor- and acceptor-tagged molecules cannot be controlled, such as in cellular studies.

Materials and Methods

Materials

1-Palmitoyl-2-oleoyl-*sn*-glycero-3-phosphocholine (POPC) was purchased from Avanti (Birmingham, AL). The 33-amino acid-long TM domain of FGFR3 (TM_{WT}, sequence RRAGSVYAGILSYGV**G**FFLFILVVAAVTLCRLR, and the pathogenic mutant TM_{382Asp}, sequence RRAGSVYAGILSYGV**D**FFLFILVVAAVTLCRLR) were synthesized using solid-phase peptide synthesis, as described previously (Li, You and Hristova 2006; Iwamoto et al. 2005). The peptides were purified using reverse-phase high-performance liquid chromatography (HPLC; Varian Analytical Instruments, Walnut Creek, CA) using a water/acetonitrile gradient. Matrix Assisted Laser Desorption/Lonization-Time of Flight mass spectrometry confirmed the correct molecular weight of the peptides. The single Cys residue in the peptide was labeled with fluorescein-maleimide (donor) and rhodamine-maleimide (acceptor) (Molecular Probes, Eugene, OR) and purified as previously described (Li et al. 2005; Li and Hristova 2004).

Vesicle Preparation and FRET Measurements

Lipids in chloroform and peptides in hexafluoro-2-propanol were mixed, as described (You et al. 2005). The organic solvents were removed under a steam of nitrogen gas; the mixture was lyophilized and then redissolved in 10 mM phosphate buffer and 500 mM NaCl (pH 7) to a concentration of 0.25 mg/ml of lipids. Samples were freeze-thawed several times before the FRET experiments, as discussed in detail elsewhere (You et al. 2005).

Emission and excitation spectra of labeled peptides in vesicles were measured using a Fluorolog 3–22 fuorometer (Jobin Yvon, Edison, NJ). The vesicle solution was placed in a 10 × 2 mm quartz cuvette (Starna Cells, Atascadero, CA). For the emission scans, the excitation wavelength was set at 439 nm and the emission intensity was collected at 450–700 nm. In the excitation scans, the emission intensity was collected at 595 nm and the excitation wavelength was scanned at 400–570 nm.

The EmEx-FRET Method

Overview

The method that we introduce, EmEx-FRET, relies on the acquisition of both excitation and emission spectra for the ''FRET sample,'' i.e. the liposomal solution containing both donor-labeled and acceptor-labeled TM helices. Furthermore, both excitation and emission spectra need to be acquired for donor-only and acceptor-only ''standards'' of well-known donor and acceptor concentrations. In the EmEx-FRET method, we rely on these standard spectra to calculate not only the FRET efficiency but also the actual donor and acceptor concentration and, therefore, the equilibrium constants and the free energy of lateral dimerization with high experimental precision. As discussed below, uncertainties in actual donor and acceptor concentrations, due to sample-to-sample variations as a result of low peptide solubility, can be resolved and just a few spectra are sufficient to reliably determine the energetics of interactions.

Theory

The efficiency of energy transfer, E, from an excited donor to an acceptor is defined as follows (Lakowicz 1999):

$$E = 1 - \frac{F_{DA}\left(\lambda_{em}^{D}\right)}{F_{D}\left(\lambda_{em}^{D}\right)} \tag{1}$$

where F_{DA} and F_D denote the donor emission in the presence and in the absence of an acceptor, respectively, and λ_{em}^{D} is the wavelength of the maximum donor emission (*see* Fig. 1B). Similarly, F_{AD} and F_A will be used to denote the acceptor emission in the presence and in the absence of a donor. F_{DA} (just as F_D, F_A, F_{AD}, etc.) denotes the complete emission spectra, while $F_{DA}(\lambda_{em}^{D})$ refers to the fluorescence intensity value at λ_{em}^{D}.

When both the donor and the acceptor are present, we can write the following:

$$F_{DA}\left(\lambda_{em}^{D}\right) = S_D\left[\varepsilon_D\left(\lambda_{ex}^{D}\right)\cdot[d] - \varepsilon_D\left(\lambda_{ex}^{D}\right)\cdot[d]\cdot E\right] \tag{2}$$

$$F_{AD}\left(\lambda_{em}^{A}\right) = S_A\left[\varepsilon_A\left(\lambda_{ex}^{D}\right)\cdot[a] + \varepsilon_D\left(\lambda_{ex}^{D}\right)\cdot[d]\cdot E\right] \tag{3}$$

where $[d]$ and $[a]$ are the donor and acceptor concentrations in the sample, $\varepsilon_D\left(\lambda_{ex}^{D}\right)$ and $\varepsilon_A\left(\lambda_{ex}^{D}\right)$ are the extinction coefficients of the donor and the acceptor at λ_{ex}^{D} (*see* Fig. 1), S_D and S_A are scaling factors which depend on the quantum yields of the donor and acceptor, the photodetector efficiencies at λ_{em}^{D} and λ_{em}^{A} and the geometry of the experimental setup. At zero FRET efficiency ($E = 0$), the donor and the acceptor emit due to direct excitation only, such that $F_{DA} = F_D$ and $F_{AD} = F_A$. At non-zero FRET efficiency ($E \neq 0$), part of the energy, absorbed by the donor, is transferred to the acceptor. The donor fluorescence is quenched ($F_{DA} < F_D$), and the acceptor fluorescence is enhanced ($F_{AD} > F_A$). The acceptor enhancement, termed ''sensitized fluorescence'' (F_{sen}), can be calculated as follows:

$$\begin{aligned} &F_{sen} = F_{AD} - F_A \\ &F_{sen}\left(\lambda_{em}^{A}\right) = S_A \cdot \varepsilon_D\left(\lambda_{ex}^{D}\right)\cdot[d]\cdot E \end{aligned} \tag{4}$$

The donar quenching is given by the following:

$$\begin{aligned} &\Delta F_D = F_D - F_{DA} \\ &\Delta F_D\left(\lambda_{em}^{D}\right) = S_D\cdot\varepsilon_D\left(\lambda_{ex}^{D}\right)\cdot[d]\cdot E = F_{sen}\left(\lambda_{em}^{A}\right)\cdot\frac{S_D}{S_A} \end{aligned} \tag{5}$$

Therefore, the efficiency of donor quenching at λ_{em}^{D} is proportional to the sensitized acceptor fluorescence at λ_{em}^{A}, with S_D/S_A being the scaling factor.

The scaling factor S_D/S_A depends on the dyes used and on the characteristics of the instrument, not on the particular dye concentration. S_D/S_A can be calculated from the FRET spectrum in a system of well-defined dye concentrations and known FRET efficiency according to the following:

$$\frac{S_D}{S_A} = \frac{\Delta F_D\left(\lambda_{em}^{D}\right)}{F_{sen}\left(\lambda_{em}^{A}\right)} \tag{6}$$

Alternatively, if the photodetector efficiency at λ_{em}^{D} and λ_{em}^{A} is the same (or if the fluorescence signal is normalized by the photodetector efficiency), then S_D/S_A equals the ratio of donor and acceptor quantum yields, φ_D/φ_A, which can be calculated from measured absorbance and emission spectra.

Once S_D/S_A is determined, it can be used to calculate the donor fluorescence in the absence of the acceptor (i.e., the donor control, F_D) from the measured donor fluorescence in the presence of the acceptor F_{DA} according to the following:

$$F_D\left(\lambda_{em}^{D}\right) = F_{DA}\left(\lambda_{em}^{D}\right) + F_{sen}\left(\lambda_{em}^{A}\right)\cdot\frac{S_D}{S_A} \tag{7}$$

The Donor and Acceptor Standards

Figure 1 shows the excitation and the emission spectra of the fluorescein/rhodamine FRET pair, conjugated to the WT FGFR3 TM domain. The amplitudes of these spectra depend on the total three-dimensional (3D) concentration of the fluorophores (i.e., moles of labeled peptides per unit volume). The FRET efficiencies and the dimerization

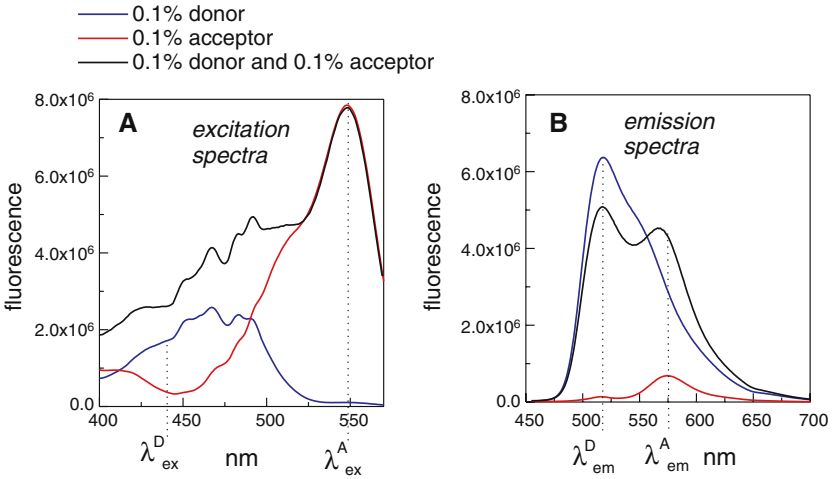

Fig. 1 Emission and excitation spectra of fluorescein (Fl) and rhodamine (Rhod), a common FRET pair, conjugated to TM_{WT}. POPC concentration was 0.25 mg/ml; the concentration of the protein is reported in moles of protein per mole of lipid. (*A*) Excitation spectra collected by recording emission at 595 nm while scanning the excitation at 400–570 nm. (*B*) Emission spectra. Excitation was fixed at 439 nm, and emission was scanned at 450–700 nm. In *A* and *B*, *blue lines* correspond to 0.1 mol% Fl-TM_{WT} and *red lines* are for 0.1 mol% Rhod-TM_{WT}. Blue and red spectra serve as standard excitation and emission spectra, to be used with the EmEx-FRET method. These spectra are averages, derived from measurements of multiple samples, prepared as described in Materials and Methods. Also shown are the excitation and emission spectra of 0.1 mol% Fl-TM_{WT} and 0.1 mol% Rhod-TM_{WT} (the donor/acceptor sample, or ''FRET sample,'' *black lines*). The FRET spectrum (*black*) is the sum of three contributions: direct donor emission in the presence of the acceptor F_{DA}, direct acceptor emission F_A and sensitized acceptor emission F_{sen}. Inspection of the excitation spectra in *A* reveals that at excitation wavelength λ^A_{ex} the acceptor excitation reaches its maximum, while the donor excitation is negligible. As a result, the excitation of the donor/acceptor sample (*black*) at λ^A_{ex} is contributed by the acceptor only (*red*). λ^D_{ex} = 439 nm is the excitation wavelength used in the acquisition of the emission spectra. In *B*, the emissions of the donor and the acceptor reach their maxima at λ^D_{em} and λ^A_{em}, respectively. Note that the emission of the acceptor is low, but not negligible, at λ^D_{em}

energetics in liposomes, however, are determined solely by the protein-to-lipid ratio (You et al. 2005). Therefore, experiments could be carried out at various protein and lipid 3D concentrations and then interpreted with respect to the protein-to-lipid ratio. Alternatively, all experiments can be performed at fixed lipid 3D concentration, by varying the protein concentration (the protein-to-lipid ratio). The latter is the approach that we have taken in this work. In all experiments, the lipid concentration was fixed at 0.25 mg/ml (0.325 mmolar POPC solution). The protein concentration was varied and is reported in mol% (moles of protein per mole of lipid).

The blue lines in Figure 1 were recorded for 0.1 mol% Fl-TM_{WT}, while the red lines are for 0.1 mol% Rhod-TM_{WT}. Inspection of the excitation spectra in Figure 1A reveals that at excitation wavelength λ^A_{ex} the acceptor excitation reaches its maximum, while the donor excitation is negligible. Thus, the fluorescence of the acceptor at λ^A_{ex} in the presence and absence of the donor is the same (i.e., the black and the blue spectra coincide at λ^A_{ex}; *see* Fig. 1A). This spectral feature is crucial for the applicability of the EmEx-FRET method. We point out that this is a feature of many FRET pairs, such as Cy3 and Cy5, YFP and Cherry, etc. Thus, the EmEx-FRET method that we introduce is not restricted to fluorescein and rhodamine but has a broad utility.

The excitation and emission spectra of the donor only (blue lines) and acceptor only (red lines) in Figure 1 are used as ''standard'' spectra in the EmEx-FRET method and are referred to as ''excitation and emission standards.'' The amplitudes of the standard spectra should be known with high accuracy. Therefore, multiple measurements at different dye concentrations are recommended to generate these standards. The spectra of the fluorophores are usually environment-sensitive, and the standard spectra should be acquired under exactly the same conditions (pH, lipid composition, etc.) as those used for acquisition of the FRET spectra. Once the standard spectra are available, the spectrum of every sample containing both donor and acceptor (i.e. every ''FRET sample'') can be used to calculate the actual donor and acceptor concentrations in the sample, the FRET efficiency and the free energy of interactions using the EmEx-FRET protocol described below.

The EmEx-FRET Protocol

Step 1 A solution of liposomes containing donor-labeled and acceptor-labeled TM domains (i.e. a ''FRET sample'') was prepared as previously described (You et al. 2005), and the excitation and emission spectra were acquired as discussed in Materials and Methods. Each FRET spectrum

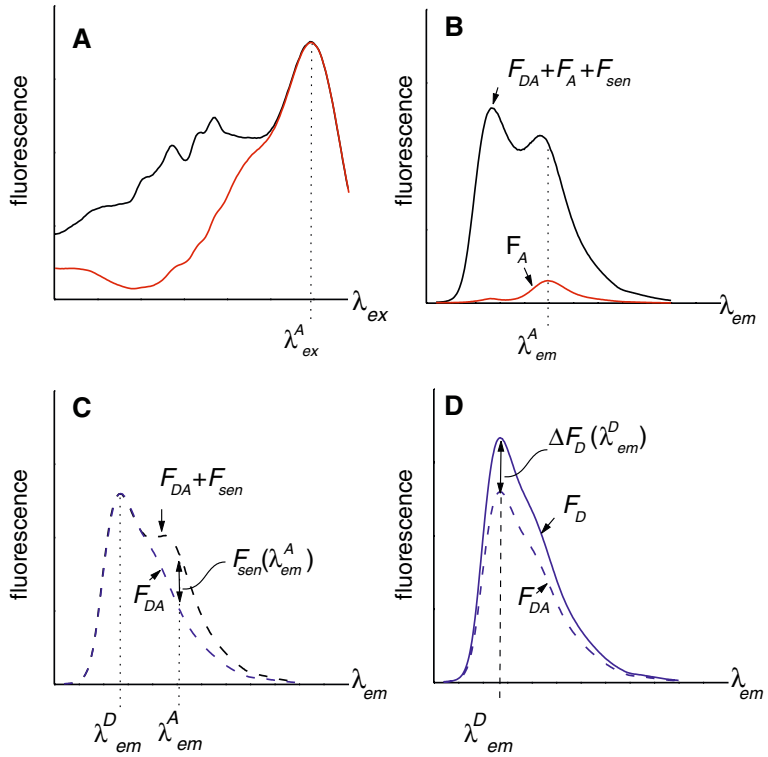

Fig. 2 The EmEx-FRET method. (*A*) An acquired FRET excitation spectrum (*black line*) is compared to the excitation standard spectrum of the acceptor (Fig. 1A, red line). This step gives the concentration of the acceptor in the sample. (*B*) The emission standard of the acceptor (Fig. 1B, red line) is scaled according to the acceptor concentration determined in *A* (*red line*). The difference between the red line and the FRET emission spectrum (*black line*) is the sum $F_{DA} + F_{sen}$. (*C*) *Dashed black line*, $F_{DA} + F_{sen}$, sum of the direct donor emission in the presence of the acceptor, $F_{DA,}$ and the sensitized acceptor emission, F_{sen}. The standard emission spectrum of the donor (Fig. 1B, blue line) is scaled such that the amplitude of the scaled standard (*blue dashed line*) is identical to the amplitude of the *dashed black line* at λ^A_{em}. The difference between the *black* and *blue dashed lines* is the sensitized acceptor emission, F_{sen}. The value of the sensitized emission at λ^A_{em}, $F_{sen}(\lambda^A_{em})$, is related to the decrease in donor emission at λ^D_{em}, $\Delta F_D(\lambda^D_{em})$ (Eq. 5). (D) The value $\Delta F_D(\lambda^D_{em})$, determined in *C*, is used to determine the donor emission in the absence of the acceptor F_D (*blue line*) and the donor concentration

(i.e., the spectrum of the FRET sample) has three contributions: direct donor emission in the presence of the acceptor F_{DA}, direct acceptor emission F_A and sensitized acceptor emission F_{sen}. Furthermore, $F_{AD} = F_A + F_{sen}$.

Step 2 The acquired FRET excitation spectrum (Fig. 2A, black line) is compared to the standard excitation spectrum of the acceptor (Fig. 1A, red line). The standard spectrum is multiplied by a coefficient, ξ, to produce the red line in Figure 2A, such that the amplitude of the scaled standard (Fig. 2A, red line) is identical to the FRET excitation spectrum (Fig. 2A, black line) at λ^A_{ex} This step gives the concentration of the acceptor in the sample, $[a]$, as ξ times the standard acceptor concentration, in this case $\xi \times 0.1$ mol%.

Step 3 The emission standard of the acceptor (Fig. 1B, red line) is multiplied by ξ to obtain the direct emission contribution of the acceptor (Fig. 2B, red line). The direct acceptor contribution (red line) is subtracted from the FRET emission spectrum (Fig. 2B, black line), to reveal the sum of the direct donor emission and the sensitized acceptor emission, $F_{DA} + F_{sen}$. This sum is plotted in Figure 2C with the black dashed line.

Step 4 The emission standard spectrum of the donor (Fig. 1B, blue line) is multiplied by a coefficient to produce the blue dashed line in Figure 2C, such that the amplitude of the scaled standard (blue dashed line) is identical to the black dashed line in Figure 2C at $\lambda^D_{em.}$ The difference between the black dashed and the blue dashed line is the sensitized acceptor emission, F_{sen}. The value of the sensitized emission at λ^A_{em}, $F_{sen}(\lambda^A_{em})$, is related to the decrease in donor emission at λ^D_{em}, $\Delta F_D(\lambda^D_{em})$, given by Eq 5.

Step 5 The value $\Delta F_D(\lambda^D_{em})$, determined in step 4, is added to $F_{DA}(\lambda^D_{em})$ (Fig. 2D) to give the value of the donor emission in the absence of acceptor at λ^D_{em}, i.e., $F_D(\lambda^D_{em}) = \Delta F_D(\lambda^D_{em}) + F_{DA}(\lambda^D_{em})$. The donor emission standard (Fig. 1B, blue line) is multiplied by coefficient ζ,

such that the amplitude of the standard spectrum at λ_{em}^{D} equals $F_D(\lambda_{em}^{D})$. This step gives the concentration of the donor in the sample, $[d]$, as ζ times the standard donor concentration, in this case $\zeta \times 0.1$ mol%. It also gives the complete emission spectrum of the donor in the absence of the acceptor F_D (Fig. 2D, blue line) as the emission of the donor standard (Fig. 1B, blue line) multiplied by ζ. The FRET efficiency is calculated from $F_D(\lambda_{em}^{D})$ and $F_{DA}(\lambda_{em}^{D})$ using Eq 1.

Thus, we determine not only the FRET efficiency (step 5) but also the donor concentration (step 5) and the acceptor concentration (step 1).

Further Data Analysis

Knowledge of the FRET efficiency and the donor and acceptor concentrations allows calculation of equilibrium constants describing TM helix dimerization. As discussed previously (You et al. 2005), the measured FRET efficiency, E, has two contributions, one due to random colocalization of donors and acceptors (proximity effects) and one due to sequence-specific interactions:

$$E = E_{proximity} + E_{oligomer} \tag{8}$$

The FRET efficiency due to the proximity effect, $E_{proximity}$, is a function of the acceptor concentration $[a]$ and can be calculated as outlined in detail elsewhere (Li et al. 2005; Li, You and Hristova 2006). The FRET efficiency due to specific oligomerization, $E_{oligomer}$, can be presented as follows:

$$E_{oligomer} = f_O \cdot p_D \cdot E_R \tag{9}$$

where f_O is the fraction of molecules in the oligomeric state, p_D is the probability for donor quenching in the oligomer and E_R is the FRET efficiency in the oligomer. If the oligomers are much smaller than the Förster radius, then $E_R = 1$. The probability of a donor-labeled molecule dimerizing with another donor-labeled or unlabeled molecule is $1 - x_A$, where x_A is the fraction of the acceptor-labeled molecules, $x_A = \frac{[a]}{[d]/f_d + [a]/f_a}$, and f_d and f_a are the donor and acceptor labeling yields. The probability of a donor-labeled molecule oligomerizing only with donor-labeled or unlabeled molecules is $(1 - x_A)^{n-1}$, where n is the number of molecules in the oligomer. Any donor will be quenched if it oligomerizes with at least one acceptor and therefore:

$$p_D = 1 - (1 - x_A)^{n-1} \tag{10}$$

Since $[a]$ and $[d]$ can be determined using the EmEx-FRET method for each sample, $E_{proximity}$ and x_A can be calculated too, such that the fraction of molecules in the oligomeric state and the number of molecules in the oligomer can be calculated.

In the case of dimers, $n = 2$, $p_D = x_A$ and $f_O = 2[D]/[T]$, where $[D]$ is the dimer concentration and $[T]$ is the total peptide concentration. Note that all concentrations are in moles of peptide per mole of lipid (You et al. 2005), as discussed above.

Results

EmEx-FRET Method Verification

To verify the EmEx-FRET method, we used previously published data for the WT FGFR3 TM domain (Li, You

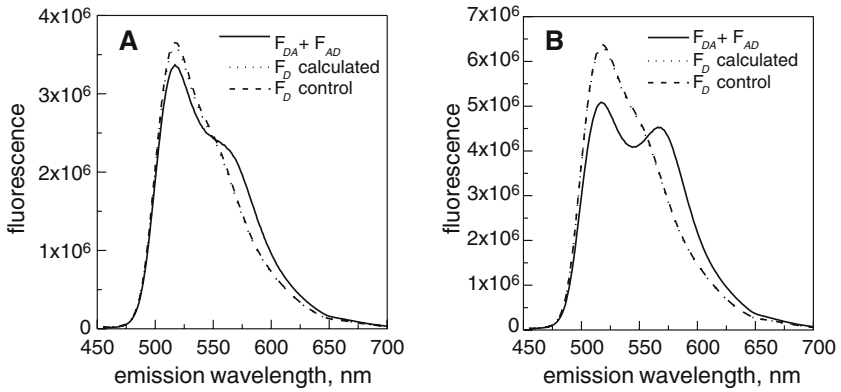

Fig. 3 Emission spectra of Fl/Rhod-labeled TM_{WT} in POPC. All experimental spectra are from a previous extended study of this protein (Li, You and Hristova 2006) and are based on multiple measurements. (*A*) *Solid line*, 0.04 mol% Fl-TM_{WT} (intended) and 0.04 mol% Rhod-TM_{WT} (intended). The actual Fl-TM_{WT} concentration is calculated as 0.0393 mol%, and the calculated donor-only control spectrum is shown with the *dotted line*. (*B*) *Solid line*, 0.1 mol% Fl-TM_{WT} (intended) and 0.1 mol% Rhod-TM_{382Asp} (intended). Fl-TM_{WT} concentration is calculated as 0.099 mol%, and the calculated donor-only control spectrum is shown with the *dotted line*. The experimental donor-only controls, shown with the *dashed lines*, are very similar to the calculated ones (*dotted lines*)

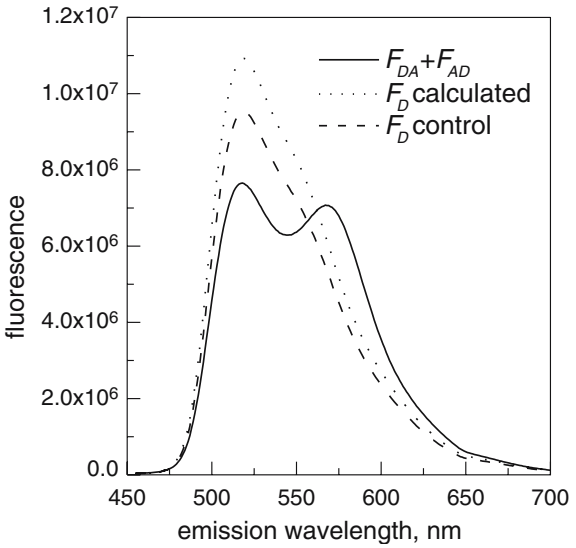

Fig. 4 A calculation of free energy of dimerization from a single FRET experiment. The intended molar concentration of both Fl-TM_{wt} and Rhod-TM_{wt} is 0.15 mol% (0.15 peptides per 100 lipids, total lipid concentration is 0.25 mg/ml). The emission spectrum (*black solid line*) is acquired by exciting at 439 nm and scanning the emission at 450–750 nm. The florescein-only control (0.15 mol% Fl-TM_{wt}, *dashed line*) is the average of multiple sample measurements. Using the experimental florescein-only control (*dashed line*) and the single FRET spectrum (*solid line*), we determine, from the decrease in donor quenching, the dimerization free energy as –1.8 kcal/mol. Using the FRET spectrum and the EmEx-FRET method, we calculate the ''actual'' concentrations of Fl-TM_{WT} and Rhod-TM_{WT} as 0.172 mol% and 0.123 mol%, respectively, and the dimerization free energy as –2.9 kcal/mol. The value from an extended experimental study, based on multiple measurements at various peptide concentrations, is –2.8 ± 0.1 kcal/mol

and Hristova 2006). The dimerization energetics for WT is well characterized, based on an extensive study comprising multiple measurements for various peptide-to-lipid ratios and donor-to-acceptor ratios. We used these data in the following way. First, we determined the ratio S_D/S_A from averaged FRET spectra for 0.08, 0.2, 0.25 and 0.3 mol% peptide, donor-to-acceptor ratio = 1, using Eq 6. Next, we used the calculated S_D/S_A and the EmEx-FRET method, as described in Materials and Methods, to analyze the FRET spectra acquired for 0.1 and 0.4 mol% peptide and calculated the anticipated donor-only control (donor fluorescence in the absence of the acceptor, F_D). Finally, the calculated donor-only control was compared to the experimental donor-only control (*see* Fig. 3).

S_D/S_A for the fluorescein-rhodamine FRET pair was determined from Eq. 6 to be 1 ± 0.05. As discussed in Materials and Methods, S_D/S_A can be determined alternatively by measuring the quantum yields of the donor and acceptor, φ_D and φ_A, at λ^D_{em} and λ^A_{em}, respectively. The quantum efficiency of the photodetector used at these wavelengths was practically the same, such that $S_D/S_A = \varphi_D/\varphi_A$. From measurements of ultraviolet absorbance and fluorescence spectra (*not shown*), we obtain $\varphi_D/\varphi_A = 1.06 \pm 0.1$, similar to a published value of $\varphi_D/\varphi_A = 1.02 \pm 0.04$ (Magde, Wong and Seybold 2002).

Based on all these measurements, a value of $S_D/S_A = 1.0$ was chosen to calculate the anticipated donor fluorescence in the absence of the acceptor from the experimental FRET spectra for 0.1 and 0.4 mol% WT. Figure 3A and B shows the experimental F_{DA} spectra (solid lines), the calculated anticipated F_D spectra (dotted lines) and the experimental F_D control spectra (dashed lines) for 0.1 and 0.4 mol% WT, respectively. Comparison of the dashed and dotted lines shows that the calculated F_D spectra are within 2% of the experimental donor-only controls, validating the EmEx-FRET method.

We further showed that the EmEx-FRET method allows accurate calculation of the free energy of dimerization, even from a single experiment. A FRET spectrum (solid line) and an experimental donor-only control (dashed line) are shown in Figure 4. The FRET spectrum was measured for a single sample, a liposomal solution with 0.15 mol% (intended) fluorescein-labeled TM_{WT} and 0.15 mol% (intended) rhodamine-labeled TM_{WT}. The calculation of the dimerization free energy based on donor quenching from the two experimental spectra in Figure 4, a method that we have used previously to calculate the free energy of dimerization (You et al. 2005), gives –1.8 kcal/mol (the detailed protocol for such calculations has been published elsewhere [Li et al. 2005; Li, You and Hristova 2006; You et al. 2005]). This value is different from the value obtained in an extended experimental study, based on multiple measurements at various peptide concentrations, –2.8 ± 0.1 kcal/mol (Li, You and Hristova 2006). Using the FRET emission spectrum (solid line), the FRET excitation spectrum (*not shown*) and the EmEx-FRET method, we determined the ''actual'' concentrations of FL-TM_{WT} and Rhod-TM_{WT} to be 0.172 mol% and 0.123 mol%, and we calculated the dimerization free energy as –2.9 kcal/mol, which is within experimental error of the published value of –2.8 ± 0.1 kcal/mol (Li, You and Hristova 2006).

EmEx-FRET analysis of the FRET spectrum in Figure 4 demonstrates that the fluorophore concentrations in the sample are different from the intended 0.15 mol%. As a result, the donor-to-acceptor ratio is 1.4 instead of 1, thus affecting the free energy calculations. Furthermore, the experimental florescein-only control (dashed line) is not the appropriate one since the concentration of the donor in the ''FRET sample'' is higher than intended. The incorrect donor and acceptor concentrations and the improper florescein-only control lead to an inaccurate free energy calculation, –1.8 kcal/mol. The basis of the error is the limited experimental precision in the preparation of samples of well-defined donor and acceptor concentrations, due to

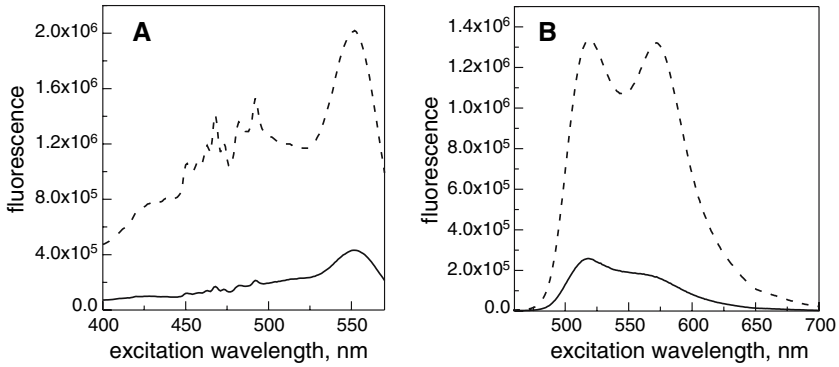

Fig. 5 Fluorescence spectra of Fl/Rhod-labeled TM_{382Asp} in POPC. POPC concentration was 0.25 mg/ml. (*A*) Excitation spectra. (*B*) Emission spectra. *Solid lines*, 0.025 mol% Fl-TM_{382Asp} (intended) and 0.025 mol% Rhod-TM_{382Asp} (intended). The actual concentrations were 0.0212 mol% (Fl-TM_{382Asp}) and 0.029 mol% (Rhod-TM_{382Asp}). *Dashed lines*, 0.15 mol% Fl-TM_{382Asp} (intended) and 0.15 mol% Rhod-TM_{382Asp} (intended). The actual concentrations were 0.149 mol% (Fl-TM_{382Asp}) and 0.135 mol% (Rhod-TM_{382Asp}). Samples were prepared as described in Materials and Methods

sample-to-sample variation and/or incomplete solubilization of the very hydrophobic peptides. However, the actual concentrations of donor- and acceptor-labeled peptides and the appropriate donor-only control (dotted line) can be calculated using the EmEx-FRET method, thus yielding the correct dimerization free energy.

Dimerization Energetics of Gly382Asp FGFR3 TM Domain

Next, we investigated the effect of the Gly382Asp mutation, identified in the KSM-18 myeloma cell line (Otsuki et al. 1998), on the dimerization propensity of FGFR3 TM domain. While cellular studies have produced contradictory results about the effect of the mutation on receptor activation (Ronchetti et al. 2001), biophysical studies of the mutant Gly382Asp TM domain have never been carried out. Here, we characterized the dimerization energetics of the mutant TM domain, TM_{382Asp}, and compared it to published data for WT (Li, You and Hristova 2006).

POPC liposomes containing donor- and acceptor-labeled TM_{382Asp} were prepared as described in Materials and Methods. Experiments were set up with total TM_{382Asp} concentrations varying between 0.05 and 0.5 mol%, a concentration range shown to be optimal for FRET measurements (Li et al. 2005; You et al. 2005). Altogether, six different FRET samples were prepared at various peptide-to-lipid ratios, donor-to-acceptor ratio = 1, and both emission and excitation spectra were acquired for all of them. Figure 5 shows the ''raw'' fluorescence spectra for two different TM_{382Asp} concentrations. From such spectra, the FRET efficiencies, E, and the actual donor and acceptor concentrations, $[d]$ and $[a]$, were determined using the EmEx-FRET method; the actual concentrations were within 20% of the intended ones. For the EmEx-FRET calculations, we used $S_D/S_A = 1$ and the donor and acceptor standards established for the WT FGFR3 TM domain. To obtain FRET that is due to sequence-specific dimerization, the contribution from random colocalization, $E_{proximity}$, was calculated as described in detail elsewhere (You et al. 2005) and subtracted from the measured FRET efficiency to give FRET due to sequence-specific dimerization, E_{dimer} (Eq. 8). We emphasize that the two contributions to the measured FRET efficiencies, one due to specific interactions and one due to random dye colocalization, can be separated only when the acceptor concentration is accurately known.

The dimer fraction $[D]/[T]$ for TM_{382Asp} was determined using Eq. 9 for $E_R = 1$, corresponding to 100% energy transfer efficiency from the donor to the acceptor in the dimer (You et al. 2005). The dimer fraction, as a function of total peptide concentration, is shown in Figure 6. The free energy of dimerization, calculated according to $\Delta G = -RT \ln K$, is –2.78 ± 0.04 kcal/mol. This value is the same as the one determined for WT, –2.8 ± 0.1 kcal/mol (Li, You and Hristova 2006), indicating that the Gly382Asp mutation does not stabilize the FGFR3 TM domain dimer.

We note that each symbol in Figure 6 shows the result from a single experiment. Yet, one can have high confidence in the data because the donor and acceptor concentrations, and therefore the total peptide concentrations, were determined using the EmEx-FRET method. Calculation of dimerization free energies from donor quenching (i.e., not using the EmEx-FRET method) gives –2.9 ± 0.7 kcal/mol. Thus, application of the EmEx-FRET method reduces the uncertainty in the free energy calculation from ± 0.7 to ± 0.04 kcal/mol and therefore increases the experimental precision.

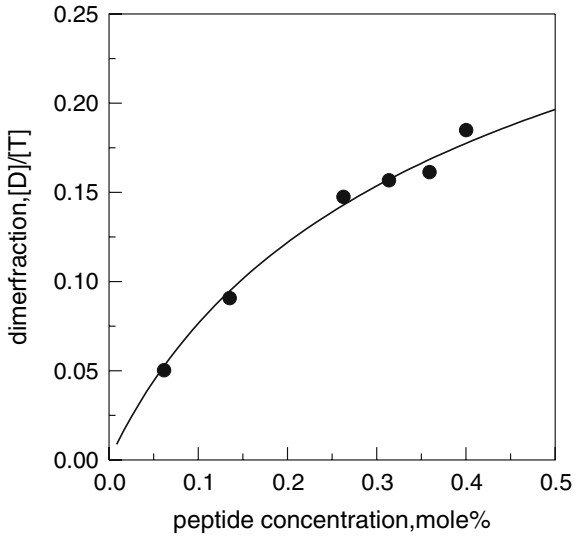

Fig. 6 Dimer fraction [D]/[T] *vs.* total peptide concentration [T] for TM_{382Asp}. Symbols represent the dimer fractions calculated using the EmEx-FRET method, for different protein concentrations. *Solid line* is the theoretical equilibrium curve, obtained as described in detail previously (Li et al. 2005; Li, You and Hristova 2006). The free energy of dimerization, as the average of the six experiments, is –2.78 ± 0.04 kcal/mol. For comparison, the average free energy value, obtained from donor quenching as previously described (You et al. 2005) (i.e., not using the EmEx-FRET method), is –2.9 ± 0.7 kcal/mol. Thus, the EmEx-FRET method increases the precision of TM helix dimerization energetics measurements

Discussion

The EmEx-FRET Method

Equilibrium constants describing TM helix interactions have been previously measured by acquiring either emission (Li et al. 2005; Li, You and Hristova 2006; You et al. 2006; Merzlyakov et al. 2006) or excitation (Fisher, Engelman and Sturgis 1999) FRET spectra. Experimental challenges can arise because the concentration of donors and acceptors cannot be verified in the ''FRET samples'' (dye:lipid ratios never exceed 1/500 and absorbance measurements lack the requisite sensitivity). Therefore, sample-to-sample variations in protein concentrations due to the very low solubility of the hydrophobic TM helices can introduce uncertainties in the measured FRET efficiencies and the calculated dimerization free energies.

The EmEx-FRET method, which gives the free energies of interactions with high precision, involves the acquisition of both emission and excitation spectra. Here, the method was verified using previously published data for the WT FGFR3 TM domain (Li, You and Hristova 2006) and used to calculate the free energy of dimerization for the Gly382Asp pathogenic FGFR3 mutant as $\Delta G = -2.78 \pm 0.04$ kcal/mol. This value was determined with high precision from single measurements at six peptide-to-lipid ratios. The actual donor and acceptor concentrations were determined for each sample, the dimer fraction was calculated using the actual donor and acceptor concentrations rather than the intended concentrations and the calculated dimer fractions were plotted as a function of the actual total peptide concentration (Fig. 6). Thus, several sources of statistical error were eliminated, resulting in high experimental precision.

We note that EmEx-FRET analysis is valid only when the fluorescence intensity of the dyes (in the absence of FRET) is linear with dye concentrations. Otherwise, self-quenching or inner filter effects, which occur at high concentrations, impair the quantitative FRET analysis. We have found that self-quenching does not occur for donor concentrations that are lower than 0.3 mol% (You et al. 2005). Therefore, dye concentrations that exceed 0.3 mol% are not recommended for measurements of TM helix dimerization using FRET.

As discussed above, the standard spectra should be acquired under exactly the same conditions (pH, lipid composition, etc.) as the ones used for the acquisition of FRET spectra. It should be further noted that spectra of free fluorophores cannot be used as standard spectra since they may be altered when the dyes are coupled to the proteins and embedded in the membrane.

The EmEx-FRET method presented here can be useful in cases when the donor and acceptor concentrations, and the total protein concentration, are not controlled or are unknown. Such a situation occurs in cellular studies, when expression of the donor-tagged and acceptor-tagged proteins cannot be controlled. Previously, unknown concentrations have been estimated by photobleaching of the acceptor (Raicu et al. 2005) or of the donor, such that FRET is ''turned off.'' The resulting changes in F_{DA} and F_{AD} can be linked to the actual initial F_D and F_A values and to the initial FRET efficiency. However, there are several potential problems with such an approach: (1) the bleaching rate of the free dyes and of dyes in the donor-acceptor complexes could be different; (2) donor and acceptor spectra are often not well separated, such that the dyes cannot be bleached independently; and (3) photoconversion during bleaching may impair further calculations. The EmEx-FRET method is free from such problems and, thus, could have applications in cases when the bleaching approach is not optimal.

The FGFR3 Gly382Asp Mutation

The Gly382Asp mutation in the TM domain of FGFR3 has been identified in the KSM–18 multiple myeloma cell line (Otsuki et al. 1998). Unlike other FGFR3 mutations, it has not been so far identified in skeletal disorders. The mutation does not affect FGFR3 activity in the KSM-18 cell line, and it is not capable of inducing foci formation in NIH

3T3 cells (Ronchetti et al. 2001). These findings are consistent with our results, which demonstrate that the mutation does not affect the dimerization energetics of FGFR3 TM domain. A previously published model of the FGFR3 TM domain, created with the software CHI (Adams et al. 1995), identifies the residues that mediate helix-helix contact to be Leu377, Val381, Phe384 and Ile387 (Li, You and Hristova 2006). In this model, Gly382 does not interact with the neighboring helix and is exposed to lipids. Based on this model, it can be expected that substitution of Gly382 with any other amino acids does not affect dimer stability, consistent with our findings. We note that the Gly382Asp mutation differs from the Crouzon Ala391Glu mutation, which stabilizes the FGFR3 TM dimer by –1.3 kcal/mol. It has been proposed that Glu in position 391 forms a hydrogen bond with the neighboring helix in the FGFR3 dimer (Li, You and Hristova 2006). However, Asp in position 382 does not appear to participate in stabilizing hydrogen bonding interactions.

Ronchetti et al. (2001) found that, in transfected 293T cells, the Asp382 mutant activates the mitogen-activated protein kinase pathway in a ligand-independent manner, while the WT required ligands. This result demonstrates that the Gly382Asp mutation is capable of causing overactivation, despite the fact that it does not stabilize the dimer. It can be therefore hypothesized that other mechanisms of pathogenesis are at play. In this respect, the Gly382Asp mutation is similar to the achondroplasia Gly380Arg mutation, which does not affect FGFR3 TM dimer stability but causes deregulated signaling.

Some RTK mutations have been shown to induce slow downregulation of the activated receptor dimers, resulting in prolonged signaling. Examples include the achondroplasia mutation in the TM domain and the thanatophoric dysplasia II Lys650Glu mutation in the catalytic domain of FGFR3 (Cho et al. 2004). Thus, dimer stabilization is not necessarily required for pathogenesis. It is possible that the Gly382Asp mutation also compromises the downregulation of FGFR3. Indeed, immunofluorescence studies of the localization of the Gly382Asp receptor have revealed intense cytoplasmic staining (Ronchetti et al. 2001).

In model bilayers, the achondroplasia mutation has been shown to induce a shift in the hydrocarbon core embedded segment of FGFR3 TM domain (X. Han et al. 2006). Based on this result, we previously hypothesized that a mutation-induced change in membrane topology may be the structural basis for the slow receptor downregulation in achondroplasia. Asp382 is not expected to participate in the dimer interface and is likely exposed to lipids, which is energetically unfavorable and may lead to changes in membrane topology. Future structural studies of the Gly382Asp mutant in bilayers, as well as cellular studies that address the fate of the Gly382Asp activated receptors, should shed further light on the role of the Gly382Asp mutation in multiple myeloma pathogenesis.

Acknowledgement We thank our colleagues Edwin Li and William C. Wimley for valuable discussions. This work was supported by NIH grant GM068619, NSF grant MCB 0315663 and Research Scholar grant RSG-04-201-01 from the American Cancer Society (to K. H.).

References

Adams PD, Arkin IT, Engelman DM, Brunger AT (1995) Computational searching and mutagenesis suggest a structure for the pentameric transmembrane domain of phospholamban. Nat Struct Biol 2(2):154–162

Blume-Jensen P, Hunter T (2001) Oncogenic kinase signalling. Nature 411:355–365

Cho JY, Guo CS, Torello M, Lunstrum GP, Iwata T, Deng CX, Horton WA (2004) Defective lysosomal targeting of activated fibroblast growth factor receptor 3 in achondroplasia. Proc Natl Acad Sci USA 101:609–614

Deng C, Wynshaw-Boris W, Zhou F, Kuo A, Leder P (1996) Fibroblast growth factor receptor 3 is a negative regulator of bone growth. Cell 84:911–921

Fantl WJ, Johnson DE, Williams LT (1993) Signaling by receptor tyrosine kinases. Annu Rev Biochem 62:453–481

Fisher LE, Engelman DM, Sturgis JN (1999) Detergents modulate dimerization, but not helicity, of the glycophorin A transmembrane domain. J Mol Biol 293:639–651

Han X, Mihailescu M, Hristova K (2006) Neutron diffraction studies of fluid bilayers with transmembrane proteins: structural consequences of the achondroplasia mutation. Biophys J 91(10):3736–3747

Iwamoto T, You M, Li E, Spangler J, Tomich JM, Hristova K (2005) Synthesis and initial characterization of FGFR3 transmembrane domain: Consequences of sequence modifications. Biochim Biophys Acta 1668:240–247

Lakowicz JR (1999) Principles of Fluorescence Spectroscopy. Kluwer Academic/Plenum Publishers, New York

Li E, Hristova K (2004) Imaging FRET measurements of transmembrane helix interactions in lipid bilayers on a solid support. Langmuir 20:9053–9060

Li E, Hristova K (2006) Role of receptor tyrosine kinase transmembrane domains in cell signaling and human pathologies. Biochemistry 45:6241–6251

Li E, You M, Hristova K (2005) SDS-PAGE and FRET suggest weak interactions between FGFR3 TM domains in the absence of extracellular domains and ligands. Biochemistry 44:352–360

Li E, You M, Hristova K (2006) FGFR3 dimer stabilization due to a single amino acid pathogenic mutation. J Mol Biol 356:600–612

Magde D, Wong R, Seybold PG (2002) Fluorescence quantum yields and their relation to lifetimes of rhodamine 6G and fluorescein in nine solvents: Improved absolute standards for quantum yields. Photochem Photobiol 75:327–334

Merzlyakov M, You M, Li E, Hristova K (2006) Transmembrane helix heterodimerization in lipids bilayers: Probing the energetics behind autosomal dominant growth disorders. J Mol Biol 358:1–7

Meyers GA, Orlow SJ, Munro IR, Przylepa KA, Jabs EW (1995) Fibroblast-growth-factor-receptor-3 (Fgfr3) transmembrane mutation in Crouzon syndrome with *Acanthosis nigricans*. Nat Genet 11:462–464

Otsuki T, Nakazawa N, Taniwaki M, Yamada O, Sakaguchi H, Wada H, Yawata Y, Ueki A (1998) Establishment of a new human

myeloma cell line, KMS-18, having t(4;14)(p16.3;q32.3) derived from a case phenotypically transformed from Ig A-lambda to BJP-lambda, and associated with hyperammonemia. Int J Oncol 12:545–552

Raicu V, Jansma DB, Miller RJD, Friesen JD (2005) Protein interaction quantified in vivo by spectrally resolved fluorescence resonance energy transfer. Biochem J 385:265–277

Ronchetti D, Greco A, Compasso S, Colombo G, Dell'Era P, Otsuki T, Lombardi L, Neri A (2001) Deregulated FGFR3 mutants in multiple myeloma cell lines with t(4;14): Comparative analysis of Y373C, K650E and the novel G384D mutations. Oncogene 20:3553–3562

Schlessinger J (2000) Cell signaling by receptor tyrosine kinases. Cell 103:211–225

Shiang R, Thompson LM, Zhu Y-Z, Church DM, Fielder TJ, Bocian M, Winokur ST, Wasmuth JJ (1994) Mutations in the transmembrane domain of FGFR3 cause the most common genetic form of dwarfism, achondroplasia. Cell 78:335–342

Vajo Z, Francomano CA, Wilkin DJ (2000) The molecular and genetic basis of fibroblast growth factor receptor 3 disorders: The achondroplasia family of skeletal dysplasias, Muenke craniosynostosis, and Crouzon syndrome with acanthosis nigricans. Endocr Rev 21:23–39

van der Geer P, Hunter T, Lindberg RA (1994) Receptor protein-tyrosine kinases and their signal transduction pathways. Annu Rev Cell Biol 10:251–337

van Rhijin B, van Tilborg A, Lurkin I, Bonaventure J, de Vries A, Thiery JP, van der Kwast TH, Zwarthoff E, Radvanyi F (2002) Novel fibroblast growth factor receptor 3 (FGFR3) mutations in bladder cancer previously identified in non-lethal skeletal disorders. Eur J Hum Genet 10:819–824

Webster MK, Donoghue DJ (1996) Constitutive activation of fibroblast growth factor receptor 3 by the transmembrane domain point mutation found in achondroplasia. EMBO J. 15:520–527

You M, Li E, Hristova K (2006) The achondroplasia mutation does not alter the dimerization energetics of FGFR3 transmembrane domain. Biochemistry 45:5551–5556

You M, Li E, Wimley WC, Hristova K (2005) FRET in liposomes: Measurements of TM helix dimerization in the native bilayer environment. Anal Biochem 340:154–164